IMPACT EFFECT ON RIGID PAVEMENT CORNER HAVING LOW SPOTS

R. K. Ghosh, Ram Lal, and S. R. Vijayaraghavan, Rigid Pavement Research Division, Central Road Research Institute, India

An approximate analysis has been made of the additional deflection that occurs in a rigid pavement corner because of the impact of a moving wheel over a low spot in the region. Analytical solutions for both supported and unsupported conditions of the corner have been presented. When there is a low spot, the dynamic deflection of the corner increases very rapidly with the speed of the vehicle up to a certain limiting speed, depending on the characteristics of the slab and support condition. In the case of thin slabs, the increase may be as high as 90 percent above the static value. In comparison, when no low spot is present, the dynamic deflection decreases with the vehicle speed and is lower than the static value. Experiments conducted for some selected cases show that the comparison between analytical and experimental values of additional dynamic deflection is satisfactory within the limitation of the investigation.

•IN RIGID PAVEMENT, surface irregularities such as low spots are sometimes observed near joints and corners. These are a result of either bad workmanship or improper maintenance. In the latter case, expulsion of sealing compound from the joints results in concentrating the stresses and impacts. The resulting localized disintegration of concrete under vehicular traffic forms depresssions or low spots. These depressions not only affect the riding quality of the pavement but also induce additional heavy impact loads on the pavement, such as the impact when a wheel travels over the low spots.

A solution for the case when the low spot is away from a joint may be obtained from Timoshenko's analysis (3). The effect of a low spot at a joint or a corner, where it is discontinuous, is covered here. The wheel load has been assumed to be concentrated at a point, and the joint has been assumed to be doweled.

FULLY SUPPORTED FORWARD SLAB

For the assumed configuration of a low spot spread over 2 diagonally opposite corners of adjacent slabs (Fig. 1), the following equation may be written with reference to the coordinates (origin O) shown in Figure 2:

$$\eta = (\lambda/2)\{1 + \cos[(2\pi x)/\iota]\} \quad (1)$$

where η is the variable depth of low spot, λ is its maximum depth at the center, and ι is its total length spread equally over both the slabs.

Reaction Due to Inertia

The effect of inertia may be neglected because the slab is fully supported and any vibration will be very much damped.

Sponsored by Committee on Flexible Pavement Design.

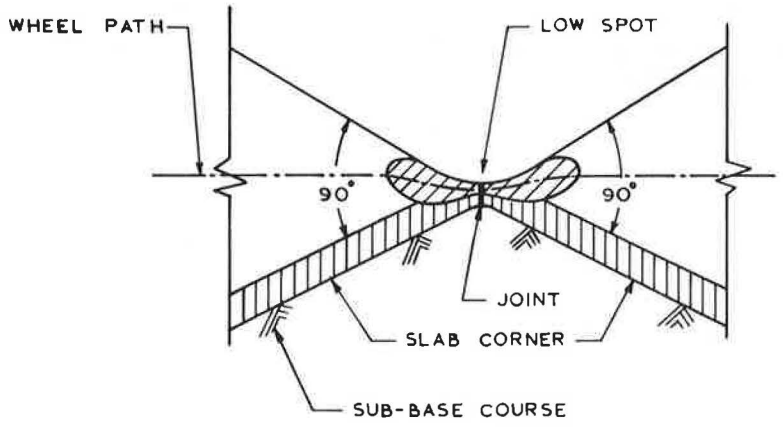

Figure 1. Low spot at adjacent slab corners of a concrete pavement.

Vertical Inertial Force of Load

If a is acceleration caused by point load W that causes additional dynamic deflection y, then

$$a = [d^2 (y + \eta)]/dt^2 \tag{2}$$

The vertical inertial force due to this acceleration is

$$F = (W/g) \{[d^2 (y + \eta)]/dt^2\} \tag{3}$$

Resisting Force Due to Elasticity

The resisting force due to the elasticity of the slab and its subgrade support is

$$R = - k \cdot y \tag{4}$$

where k is the elastic reaction modulus of the pavement system in the corner region.

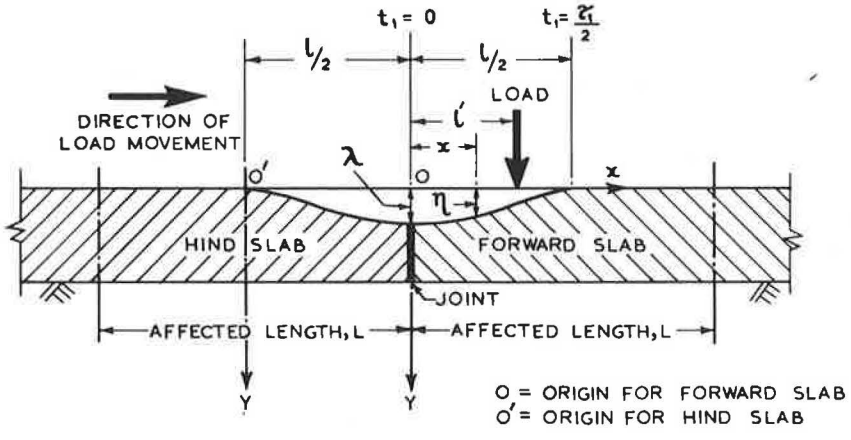

Figure 2. Section of slabs through low spot along the bisector of the corner angle.

Forced Vibration

From Eqs. 3 and 4, the equation for forced vibration due to the load moving on the low spot may be obtained as

$$(W/g)\ \{[d^2\ (y + \eta)]/dt^2\} = -k \cdot y$$

or

$$(W/g)\ (d^2y/dt^2) + ky = -(W/g)\ (d^2\eta/dt^2) \tag{5}$$

Reckoning the time from the instant the load is at x = 0 (Fig. 2) and denoting the velocity of load by υ so that $x = \upsilon \cdot t$, we obtain the following from Eq. 1:

$$\eta = (\lambda/2)\ [1 + \cos\ (2\pi\upsilon t/\iota)] \tag{6}$$

Substituting the value of η in Eq. 5, we get

$$(d^2y/dt^2) + (kg/W)\ y = (2\lambda\pi^2\upsilon^2/\iota^2)\ \cos\ (2\pi\upsilon t/\iota)$$

Denoting $kg/W = p^2$, where p is the angular frequency of free vibration, we get

$$\ddot{y} + p^2 \cdot y = (2\lambda\pi^2\upsilon^2/\iota^2)\ \cos\ (2\pi\upsilon t/\iota) \tag{7}$$

Additional Deflection

For initial conditions of y = 0 and $\dot{y} = 0$ at t = 0, the solution of Eq. 7 is obtained from Dehmul's integral (4) as

$$y = (2\lambda\pi^2\upsilon^2/p\iota^2) \int_0^{t_1} \cos\ (2\pi\upsilon t/\iota)\ \sin\ p\ (t_1 - t)\ dt$$

or

$$y = \left(\lambda/\{2[1 - (\iota^2/\upsilon^2)\ (p^2/4\pi^2)]\}\right)\ [\cos\ pt_1 - \cos\ (2\pi\upsilon/\iota)\ t_1] \tag{8}$$

Denoting $\tau_1 = \iota/\upsilon$ = total time taken by the load to cross the low spot and $\tau = 2\pi/p$ = period of free vibration, we reduce Eq. 8 to

$$y = \{\lambda/[2(1 - \tau_1^2/\tau^2)]\}\ [\cos\ (2\pi t_1/\tau) - \cos\ (2\pi t_1/\tau_1)] \tag{9}$$

For any position of the load along the low spot (Fig. 2), Eq. 9 is further modified as

$$y/\lambda = \{1/[2(1 - \tau_1^2/\tau^2)]\}\ \{\cos\ [(2\pi\iota'/\iota)\ (\tau_1/\tau)] - \cos\ (2\pi\iota'/\iota)\} \tag{10}$$

The values of y expressed in terms of λ have been calculated from Eq. 10 for different values of the ratio, τ_1/τ, corresponding to the 3 positions of load at $\iota' = \iota/4$, $3/8\ \iota$, and $\iota/2$ along the low spot. These are shown in Figure 3. Figure 3 shows that, for all values of ι', the additional deflection reaches maximum when τ_1/τ approaches zero. τ_1/τ tends to zero when the velocity of load is very high. The overall maximum occurs when ι' approaches $\iota/2$. The deflection becomes negative at locations corresponding to the values of τ_1/τ between 1 and 3.0.

Reaction Modulus

If W denotes the load (spring-borne weight), k is the elastic reaction modulus at the triangular corner, and Δ_{max} is the maximum static deflection, we get

$$k = W/\Delta_{max} \tag{11}$$

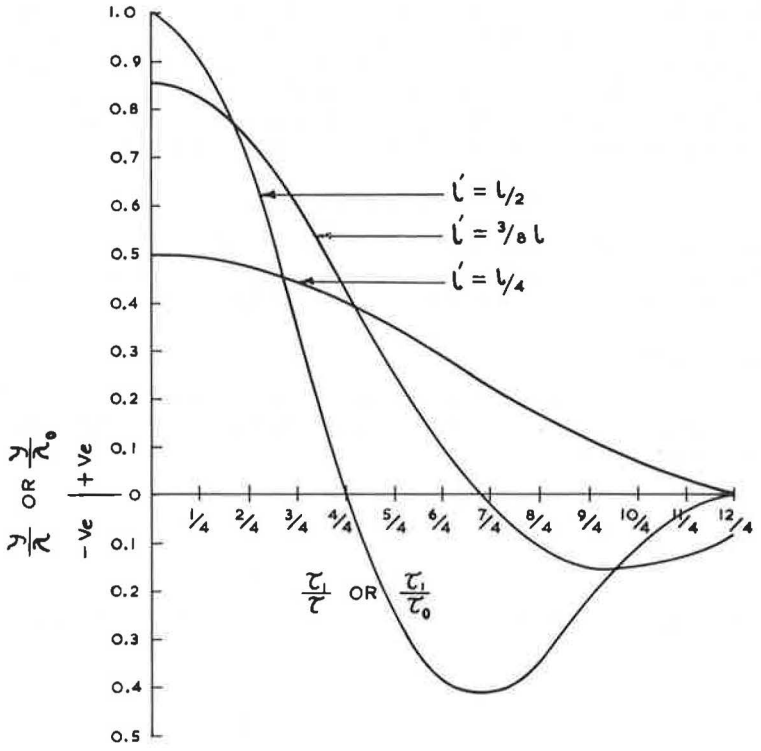

Figure 3. Additional dynamic deflection for forward slab under fully supported (y/λ vs τ_1/τ) and unsupported (y/λ_0 vs τ_1/τ_0) conditions.

The value of Δ_{max} may be computed from the following Westergaard equation (5):

$$\Delta_{max} = (W/K\iota_S^2)\,[1 \cdot 1 - (\sqrt{2} \cdot r/\iota_S)\,(0 \cdot 88)] \tag{12}$$

where K is the modulus of subgrade reaction; ι_S is the radius of relative stiffness given by $[Eh^3/12\,(1 - \mu^2)K]^{1/4}$, in which E and μ are respectively modulus of elasticity and Poisson's ratio of the slab material, and h is the slab thickness; and r is the radius of equivalent circle of tire imprint.

Neglecting r for a point load, we obtain

$$\Delta_{max} = [(1 \cdot 1\ W)/K\,\iota_S^2] \tag{13}$$

Example

If we take a particular example with W = 9,000 lb, K = 400 pci, $E = 4 \times 10^6$ psi, h = 8 in., and $\mu = 0.2$, Δ_{max} works out to be 3.78×10^{-2} in. Considering 25 percent load transfer at doweled joint, $\Delta_{max} = 0.75 \times 3.78 \times 10^{-2}$ in. The reaction modulus is $k = W/\Delta_{max} = 9{,}000/(0.75 \times 3.78 \times 10^{-2}) = 323{,}000$ lb/in. Because $p^2 = kg/W$, by substitution we get

$$p = \tfrac{1}{2\pi}\,[(323{,}000 \times 32 \times 12)/9{,}000]^{1/2} = 18.63 \text{ cps}$$

Therefore, $\tau = 1/p = {}^1/_{18.63}$ sec, and the ratio

$$\tau_1/\tau = (\iota/\upsilon)/\tau = 18.63\ \iota/\upsilon \tag{14}$$

For ι = 4, 6, and 8 in. and v ranging from 20 to 73 ft/sec (i.e., 14 to 50 mph), the values of τ_1/τ have been calculated. $(y/\lambda)_{max}$ may then be obtained from either Eq. 10 or the data shown in Figure 3. The variation of $(y/\lambda)_{max}$ with v is shown in Figure 4. It is evident that the additional downward (positive) deflection increases with the load velocity for a particular length of low spot. However, for a constant velocity, the additional downward deflection decreases with an increase in the length of low spot.

UNSUPPORTED FORWARD SLAB

In the case of an unsupported corner, the additional dynamic deflection due to a low spot being traversed by a moving load will be governed, among other factors, by the inertia of the slab, the effect of which will be appreciable.

Reaction Due to Inertia

The geometry of an unsupported corner as a cantilever slab in the form of an isosceles triangle of uniform thickness is shown in Figure 5. If the width of an elemental strip dx at a distance x from the support is

$$b_x = b\,[1 - (x/L)] \tag{15}$$

the mass of the strip is

$$w = (b_x \cdot dx \cdot h \cdot \gamma)/g \tag{16}$$

where b is the breadth of the cantilever at the support, h is the uniform slab thickness,

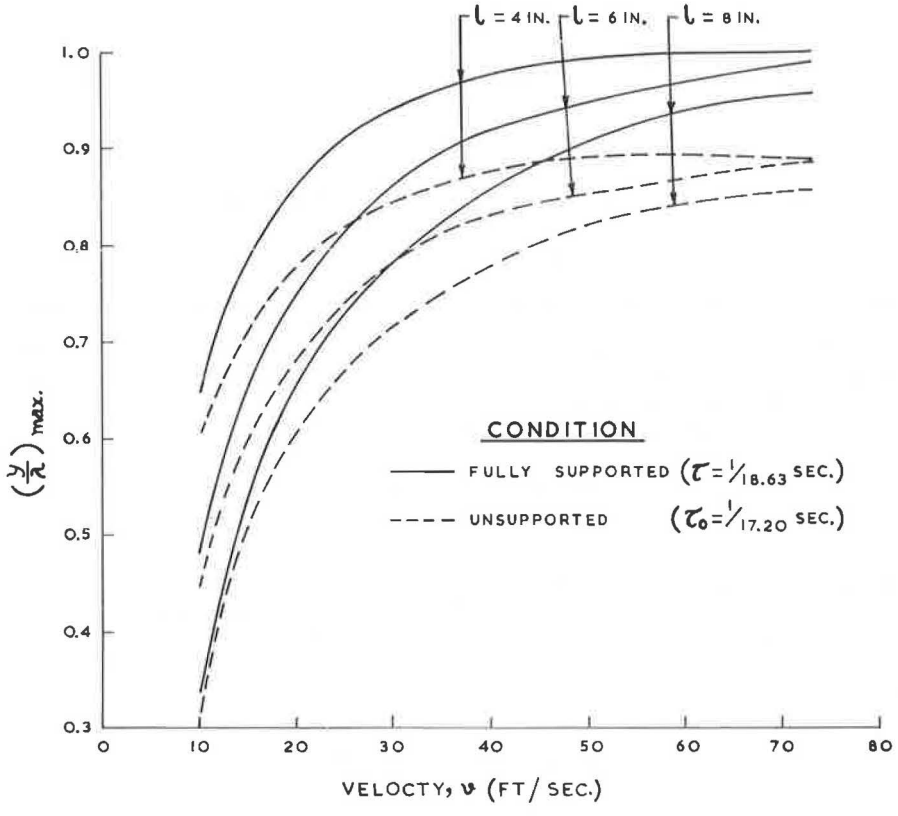

Figure 4. Maximum additional downward deflection for forward slab for different velocities of load.

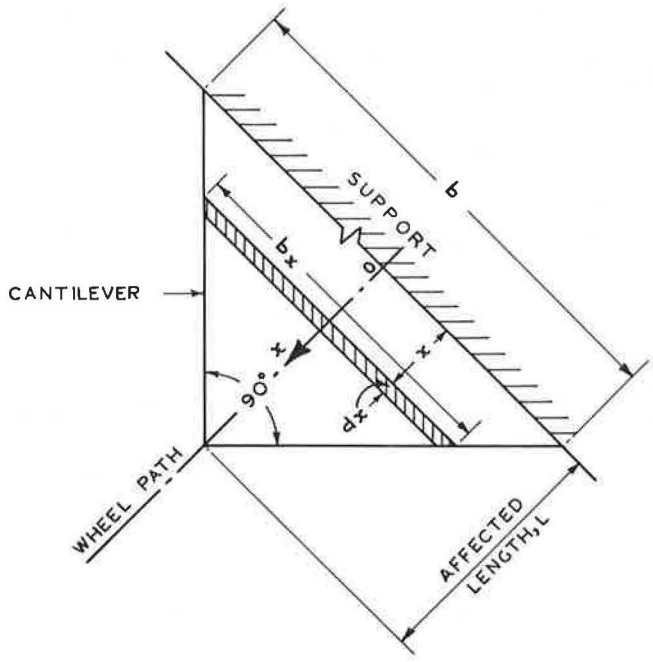

Figure 5. Unsupported corner of forward slab.

L is the unsupported effective span length of the slab, g is the acceleration due to gravity, and γ is the unit weight of slab material. Because of continuity of the cantilever over the support, the zone of influence of the load extends beyond the actually unsupported length. From tests conducted by the authors (1), it was observed that the effective length of the overhang was about 90 percent more than the actually unsupported length under both static and dynamic conditions of loading.

Because acceleration of the unit mass is equal to d^2y/dt^2, the inertial force of the strip may be obtained from

$$s_x = w(d^2y/dt^2) = [(b_x \cdot dx \cdot h \cdot \gamma)/g] (d^2y/dt^2)]$$

or

$$s_x = \left(\{b [1 - (x/L)] dx \cdot h \cdot \gamma\}/g\right) (d^2y/dt^2) \quad (17)$$

The total inertial force of the whole cantilever is, therefore,

$$S = (bh\gamma/g) (d^2y/dt^2) \int_0^L [1 - (x/L)] dx$$

or

$$S = (bh\gamma L/2g) (d^2y/dt^2) \quad (18)$$

Denoting $bh\gamma L/2 = M$, we obtain the following reaction due to inertia:

$$S = - (M/g) (d^2y/dt^2) \quad (19)$$

Vertical Inertial Force of Load

If we use the same low spot configuration as shown in Figure 2, the equation for inertial force F of the load W is

$$F = (W/g)\,\{[d^2\,(y + \eta)]/dt^2\} \tag{20}$$

Resisting Force Due to Elasticity

If we assume that the cantilever is an elastic spring, the resisting force due to its elasticity is, as before,

$$R = -\,k \cdot y \tag{21}$$

Forced Vibration

From Eqs. 19, 20, and 21, the expression for forced vibration produced by a load moving on a low spot may be obtained as

$$(W/g)\,\{[d^2\,(y+\eta)]/dt^2\} = -\,(M/g)\,(d^2y/dt^2) - k \cdot y$$

or

$$[(W + M)/g]\,(d^2y/dt^2) + k \cdot y = -\,(W/g)\,(d^2\eta/dt^2) \tag{22}$$

Applying Eq. 6 to Eq. 22, we get

$$(d^2y/dt^2) + [kg/(W + M)]\,y = [W\lambda/(W + M)]\,(2\pi^2 v^2/\iota^2)\,\cos\,(2\pi vt/\iota) \tag{23}$$

Denoting $kg/(W + M) = p_0^2$, where p_0 represents the angular frequency of free vibration and $W\lambda/(W + M) = \lambda_0$, we then transform Eq. 23 to

$$\ddot{y} + p_0^2 \cdot y = (2\lambda_0 \pi^2 v^2/\iota^2)\cos\,(2\pi vt/\iota) \tag{24}$$

Additional Deflection

For the same initial conditions as those for fully supported case, the solution of differential Eq. 24 yields

$$y = (2\lambda_0 \pi^2 v^2/p_0\,\iota^2) \int_0^{t_1} \cos\,(2\pi vt/\iota)\,\sin\,p\,(t_1 - t)\,dt$$

or

$$y = \left(\lambda_0/[2\,[1 - (\iota^2/v^2)\,(p_0^2/4\pi^2)]]\right)\,[\cos\,p_0 t_1 - \cos\,(2\pi vt_1/\iota)] \tag{25}$$

If we denote $\iota/v = \tau_1$ (as before) and $\tau_0 = 2\pi/p_0$, Eq. 25 becomes

$$y = \{\lambda_0/[2\,(1 - \tau_1^2/\tau_0^2)]\}\,[\cos\,(2\pi t_1/\tau_0) - \cos\,(2\pi t_1/\tau_1)] \tag{26}$$

For any position of load along the low spot (Fig. 2), Eq. 26 may be further modified as

$$y/\lambda_0 = \{1/[2\,(1 - \tau_1^2/\tau_0^2)]\}\,\{\cos[(2\pi\iota'/\iota)\,(\tau_1/\tau_0)] - \cos\,(2\pi\iota'/\iota)\} \tag{27}$$

Equation 27, deduced in the foregoing, is of the same form as Eq. 10. If the variation of y/λ_0 with τ_1/τ_0 for 3 positions of load (i.e., $\iota' = \iota/4$, $^3/_8\iota$, and $\iota/2$) is drawn, an exactly similar set of curves as those shown in Figure 3 would be obtained.

Reaction Modulus

As before, $\Delta_{max} = W/k$. Except for cantilever overhang (1),

$$\Delta_{max} = WL^3/2EI_0 \tag{28}$$

where I_0 represents moment of inertia of the section of the cantilever at support. Therefore,

$$k = W/\Delta_{max} = 2EI_0/L^3 \tag{29}$$

Example

If we take the same example as that for the fully supported case, then W = 9,000 lb, L (effective) = 48 in., h = 8 in., I_0 = 2,896 in.^{4}, E = 4 × 10^6 psi, and Δ_{max} (from Eq. 28) = 4.296 × 10^{-2} in. With the 25 percent load transference at doweled joints reduced, Δ_{max} = 3.22 × 10^{-2} in. From Eq. 29, the reaction modulus k = 9,000/3.22 × 10^{-2} = 279,300 lb/in. Because M = bhγL/2, taking b = $\sqrt{2}$ × 48 in. and γ = 144 lb/cu ft, we get M = 1,086 lb. Because $p_0^2 = kg/(W + M)$, we get

$$p_0 = \tfrac{1}{2}\pi\ [(279{,}000 \times 32 \times 12)/(9{,}000 + 1{,}086)]^{1/2} = 17.20 \text{ cps}$$

Therefore, $\tau_0 = {}^1/_{17.20}$ sec. But because τ_1/υ, the ratio

$$\tau_1/\tau_0 = 17.20\ \iota/\upsilon \tag{30}$$

For ι = 4, 6, and 8 in. and υ varying between 10 and 73 ft/sec (i. e., 6.82 to 50 mph), the values of the ratio τ_1/τ_0 have been computed. The values of $(y/\lambda)_{max}$ may be obtained from Figure 3. The variation of $(y/\lambda)_{max}$ with υ for the present case has been worked out and is shown in Figure 4. The set of curves obtained is similar to that for the fully supported case.

FULLY SUPPORTED HIND SLAB

Because the low spot is situated at the confluence of 2 or more slabs (Fig. 1), the moving load while traversing the low spot is met with change in support and other conditions, such as discontinuity at joints between the hind and forward slabs and slope of the low spot. Thus, as soon as the load enters the low spot in the hind slab, it begins to accelerate because of the downward slope. On approaching the forward slab, however, the load experiences a retardation with corresponding increase in pressure on the slab and, hence, deflection.

For analysis of impact effect on the hind slab, the expression for the low spot configuration may be modified as follows with reference to the origin O′ (Fig. 2):

$$\eta = (\lambda/2)\ [1 - \cos\ (2\pi x/\iota)] \tag{31}$$

Forced Vibration

The equation for forced vibration from Eq. 5 is

$$(W/g)\ (d^2y/dt^2) + k \cdot y = -\ (W/g)\ (d^2\eta/dt^2) \tag{32}$$

Reckoning the time from the instant the load is at O′ and with υ as the load velocity so that x = υt, we find from Eq. 31 that

$$\eta = (\lambda/2)\ [1 - \cos\ (2\pi\upsilon t/\iota)] \tag{33}$$

Equation 32 can now be rewritten as

$$(d^2y/dt^2) + (kg/W)\ y = -\ (2\lambda\pi^2\upsilon^2/\iota^2)\cos\ (2\pi\upsilon t/\iota) \tag{34}$$

Additional Deflection

The solution of Eq. 34 yields additional deflection as

$$y = [\lambda/[2\ (1 - \tau_1^2/\tau^2)]]\ [\cos\ (2\pi t_1/\tau_1) - \cos\ (2\pi t_1/\tau)] \qquad (35)$$

For any position of load along the centerline of the low spot, Eq. 35 may be modified as

$$y/\lambda = \{1/[2\ (1 - \tau_1^2/\tau^2)]]\ \{\cos\ (2\pi\iota'/\iota) - \cos\ [(2\pi\iota'/\iota)\ (\tau_1/\tau)]\} \qquad (36)$$

where ι' represents the distance traveled by the load at any instant measured from O'. The values of y in terms of λ have been computed from Eq. 36 for different values of τ_1/τ, and 3 positions of load at $\iota' = \iota/4$, $^3/_8\iota$, and $\iota/2$ are shown in Figure 6. It may be seen that y is negative (upward deflection) when τ_1/τ is small, i. e., velocity is high. The overall maximum positive value of 0.42λ at $\tau_1/\tau = 1.65$ is attained for y as the load approaches the corner tip of the hind slab.

For the fully supported case, $\tau_1/\tau = 18.63\ \iota/\upsilon$ (see Eq. 14). Because positive additional deflection occurs for values of τ_1/τ greater than 1, the velocities chosen for analysis range from 2.0 to 12.4 ft/sec (i. e., 1.3 to 8.4 mph) for ι = 4, 6, and 8 in. The y/λ values may be obtained from Eq. 36. The variation of $(y/\lambda)_{max}$ with υ is sinusoidal in nature and is shown in Figure 7.

UNSUPPORTED HIND SLAB

Forced Vibration

Rewriting Eq. 22 for forced vibration by substituting the value of η from Eq. 33, we get

$$(d^2y/dt^2) + [kg/(W + M)]\ y = -\ [W\lambda/(W + M)]\ (2\pi^2\upsilon^2/\iota^2)\cos\ (2\pi\upsilon t/\iota) \qquad (37)$$

Additional Deflection

Using the usual notations and solving Eq. 37, we obtain

$$y/\lambda_0 = \{1/[2\ (1 - \tau_1^2/\tau_0^2)]]\ \{\cos\ (2\pi\iota'/\iota) - \cos\ [(2\pi\iota'/\iota)\ (\tau_1/\tau_0)]\} \qquad (38)$$

Comparing Eqs. 38 and 36 shows that they are exactly alike. Therefore, the curves shown in Figure 6 representing Eq. 36 would also be valid for Eq. 38.

For the present case, the ratio $\tau_1/\tau_0 = 17.20\ \iota/\upsilon$ (see Eq. 30). For the same range of values of ι, υ, and τ_1/τ_0 as in the previous case, the maximum positive values of the ratio y/λ have been computed. The values of $(y/\lambda)_{max}$ for different values of υ are shown in Figure 7.

EXPERIMENTAL INVESTIGATION

This section discusses experimental verification of some of the analytical findings obtained previously. The experiments cover only the fully supported corner case with and without low spot.

Low Spot

Two adjacent corners at an expansion joint between concrete pavement slabs in the internal road system of the Institute were selected for the investigation. An artificial low spot, as shown in Figure 2, was prepared by grinding the concrete surface near the corners and by applying 1:1 cement-sand mortar over the ground surface. Figure 8 shows the low spot. The width and total length of the low spot were 4 and 8 in. respectively. The maximum depth, λ, was measured to be 0.10 in. at its center. Because the width of the expansion joint was $^3/_4$ in., the low spot spread over a length of $3^5/_8$ in. on each corner. The sealing compound at the joint was chamfered to conform to the general shape of the low spot.

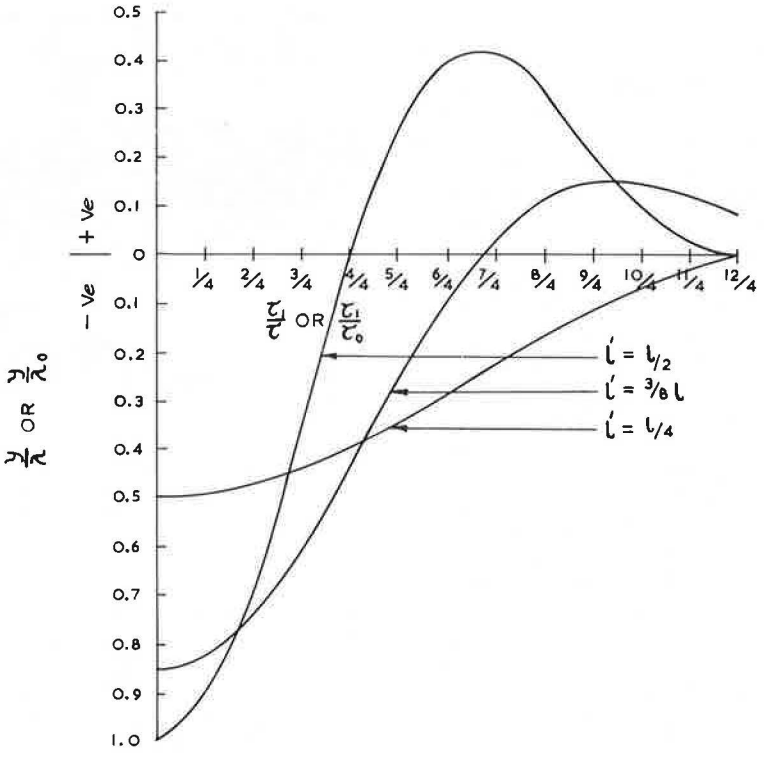

Figure 6. Additional dynamic deflection for hind slab under fully supported (y/λ vs τ_1/τ) and unsupported (y/λ_0 vs τ_1/τ_0) conditions.

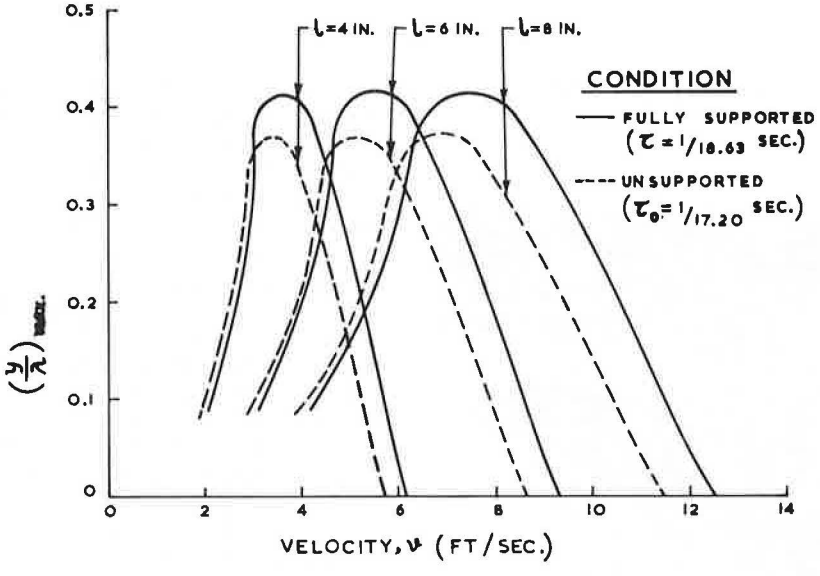

Figure 7. Maximum additional downward deflection for hind slab for different velocities of load.

Instrumentation

For measuring transient deflections caused by moving loads, a cantilever steel-strip deflectometer equipped with electrical resistance strain gages was used. Four strain gages of Hungarian Orion EMG type, each having a gage factor of 2.21 and a resistance of 120 ohms, were firmly bonded to the deflectometer, with 2 gages on each of the top and bottom surfaces at identical locations very close to the clamped end. The bridge was connected to the KWS/II-5 carrier frequency amplifier of German make (Hottinger Messtechnik). With the help of the amplifier, it was possible to have an indication of the static and dynamic responses from the movement of the recording needle. The static response could also be directly recorded through compensation by balancing the meter. The bridge-feeding was done by a 5,000 cps oscillator that also generated the switch voltage for the phase critical demodulator. The measuring voltage on the bridge output could be made visible by connecting it to a Phillips low-frequency oscilloscope. The maximum sensitivity of the oscilloscope was 2 mV/cm. The sweep time on the X-scale could be varied from 1 sec/cm to 5 μsec/cm. The vertical scale of the oscilloscope screen was calibrated for a known setting, and each small division corresponded to 0.0049 in. Figure 9 shows the general setup of the experiment.

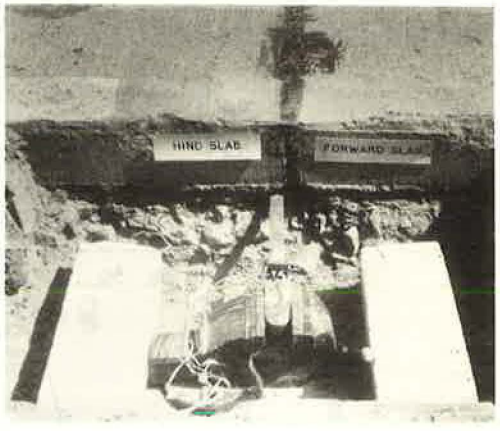

Figure 8. Test corners with low spot, with deflectometer pickup fixed under the hind slab 1 in. from center of expansion joint.

In the first series of experiments, the deflectometer tip was fixed at the bottom of the forward slab corner at a distance of 4 in. from the center of the expansion joint. In the second series, the deflectometer was placed under the hind slab corner, with its distance from the center of expansion joint being 1 in. The deflectometer assembly was protected from accidental damage during the test by being covered with a heavy steel plate.

Test Procedure

An empty Tata-Mercedes-Benz truck was used in the test. Its front and hind wheels on the right were made to traverse the test corners of 2 adjacent concrete slabs. Although the wheel load and tire pressure for both the front wheels were 2,352 lb and 82 psi respectively, those for the 2 dual-tire wheels in the rear were 2,464 lb and 84 psi respectively.

Figure 9. General setup of experiment, with amplifier and recording oscilloscope assembly shown on left.

The truck was operated to traverse the corners parallel to the longitudinal edge of the pavement at different speeds (4 to 37 mph). The static response was measured at crawl speeds of less than 1 mph. The correct position of the wheel from the edge was obtained from the tire imprint traced out by the tire on paper placed close to the corners.

The response of forward and hind slabs, with and without low spots, to a moving front wheel only was transmitted on an oscilloscope screen and photographed for each run. The dynamic deflections were computed from the photographic records

TABLE 1

LOAD TRANSFER AT JOINT UNDER STATIC LOADING CONDITION

Test	Slab That Wheel Is On	Deflection Under Load[a] (in.)	Deflection at Corner Tip of Adjacent Slab (in.)	Load Transferred (percent)
1	Forward	0.0539	0.0221	29.1
2	Forward	0.0539	0.0196	26.6
3	Forward	0.0539	0.0221	29.1
4	Hind	0.0515	0.0196	27.6
5	Hind	0.0515	0.0221	30.0
6	Hind	0.0515	0.0196	27.6
Avg				28.3

[a]When center of load is 4 in. from center of expansion point.

by measuring the peak ordinates for those runs in which the outward lateral deviation of the wheel from the longitudinal edge of the corners was 0 to 2 in. The exact speed of the truck for each run was computed from the distance between the front and rear wheels (14 ft) and the sweep time from oscilloscope records. The speedometer readings provided a rough check. Observations were also made for the static response of the forward slab corner when the front wheel was about to leave the hind slab but was still fully on it. In this position the center of load was 4 in. from the center of the expansion joint. Observations were also made of the hind slab corner with the wheel fully placed on the forward slab. From these observations, an average load transfer of 28.3 percent of wheel load at the joint could be calculated (Table 1). Responses were recorded for slabs with and without low spots.

Response of Forward Slab Without Low Spot

The maximum values of static deflection of the forward slab corner at crawl speed of the truck were recorded for different lateral positions of the front wheel. The variation in deflection for different positions of the wheel shown in Figure 10 indicated that

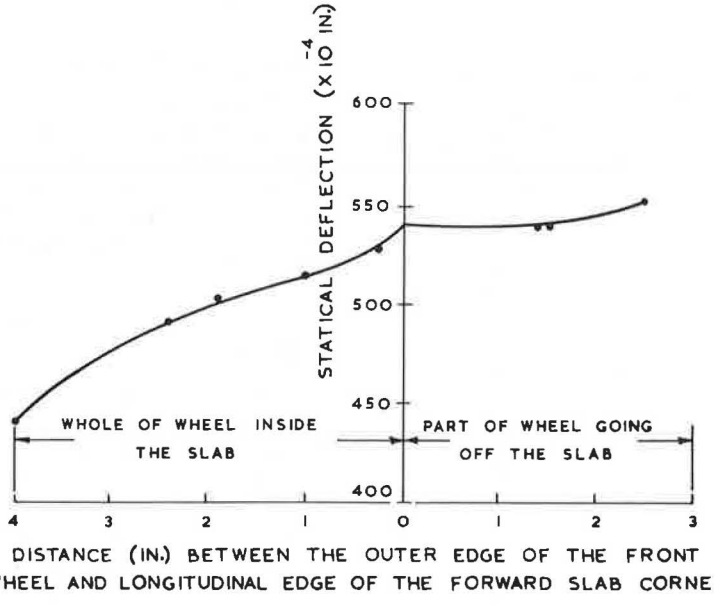

Figure 10. Variation in static deflection of the forward slab under front wheel resulting from lateral shift of latter.

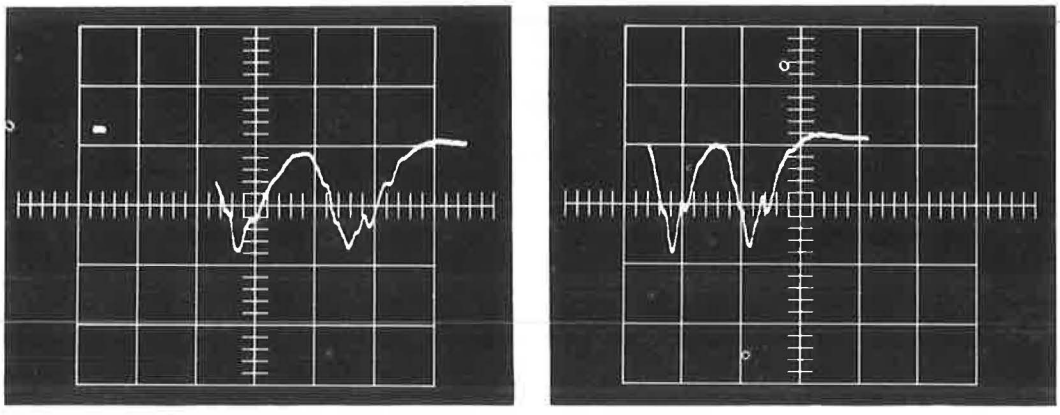

Figure 11. Kinetic response of forward slab corner without low spot: (a) speed = 39.0 ft/sec; and (b) speed = 51.5 ft/sec.

the deflection remained practically unaffected when the outer periphery of the wheel was off the edge up to 2 in. There was, however, a gradual decrease in deflection when the wheel was inside the slab but moving away from the edge.

Kinetic response of the forward slab corner was obtained by running the truck at different speeds ranging between 9.6 and 35 mph. Figure 11 shows typical photographic records of the response obtained for 2 speeds. The values of dynamic deflection for different speeds and lateral positions of the wheel are given in Table 2 and are shown in Figure 12.

Response of Forward Slab With Low Spot

In this case the truck was run at speeds between 11 and 37 mph. The typical photographic records of the responses for 2 speeds are shown in Figure 13. The test data are given in Table 2 and are shown in Figure 12.

TABLE 2

EXPERIMENTAL VALUES OF DYNAMIC DEFLECTION AT DIFFERENT SPEEDS

Slab	Test	Vehicle Speed (ft/sec)	Dynamic Deflection (in.)	Distance[a] (in.)
Forward without low spot	1	14.0	0.04655	-0.5
	2	27.5	0.04165	2.0
	3	35.0	0.04043	2.0
	4	36.8	0.03675	0.5
	5	39.0	0.03920	0.0
	6	51.5	0.03920	1.5
Forward with low spot	1	16.3	0.04900	2.0
	2	18.9	0.05390	2.0
	3	21.2	0.07105	1.0
	4	21.9	0.05880	0.0
	5	26.9	0.07350	0.0
	6	28.5	0.09065	0.5
	7	29.2	0.09310	2.0
	8	32.0	0.09675	1.0
	9	39.5	0.09675	0.0
	10	41.0	0.09800	0.0
	11	54.0	0.10535	-0.5
Hind with low spot	1	5.6	0.04655	0.0
	2	7.6	0.04900	1.0
	3	8.2	0.04900	2.0
	4	10.7	0.05390	0.5

[a]Distance of the outer periphery of the wheel from the longitudinal edge of the corner.

Response of Hind Slab

Photographic records of responses of the hind slab corner with and without low spots were obtained for speeds varying between 4 and 7 mph. A typical response record is shown in Figure 14. The results are given in Table 2 and are shown in Figure 15.

Comparison of Experimental Data With Theoretical Values

The experimental results of additional deflection were compared with the values obtained from theoretical analysis.

Reaction Modulus—For W = 2,352 lb, h = 3.7 in., K = 500 pci, μ = 0.2, and $E_{dyn} = 1.3 \times 4 \times 10^6$ psi under impact loading (30 percent increase assumed over the E_{stat} value, 2), Δ_{max} from Eq. 13 worked out to be 0.02419 in. when full load was transfered. However, because 28.3 percent of the load got transferred through

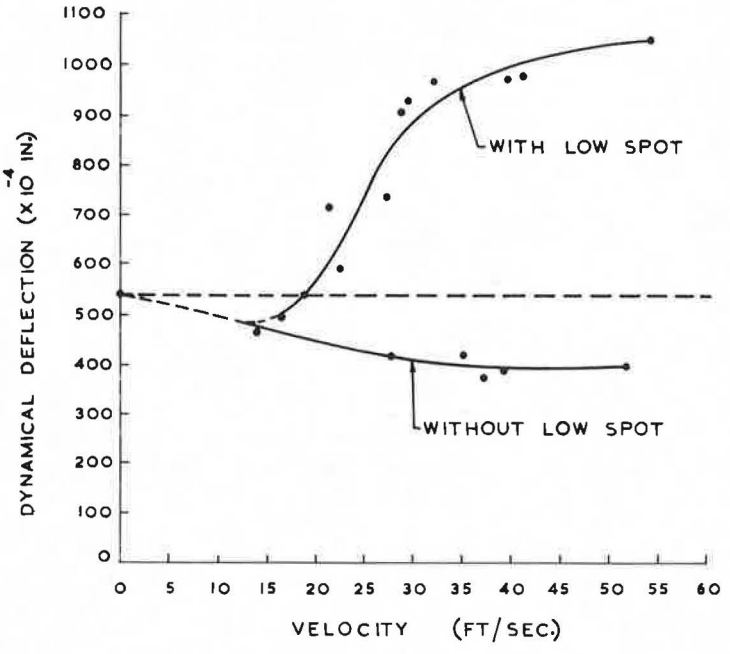

Figure 12. Experimental results of dynamic deflection of forward slab corner (at distance of 4 in. from center of expansion joint) with and without low spot for different load velocities.

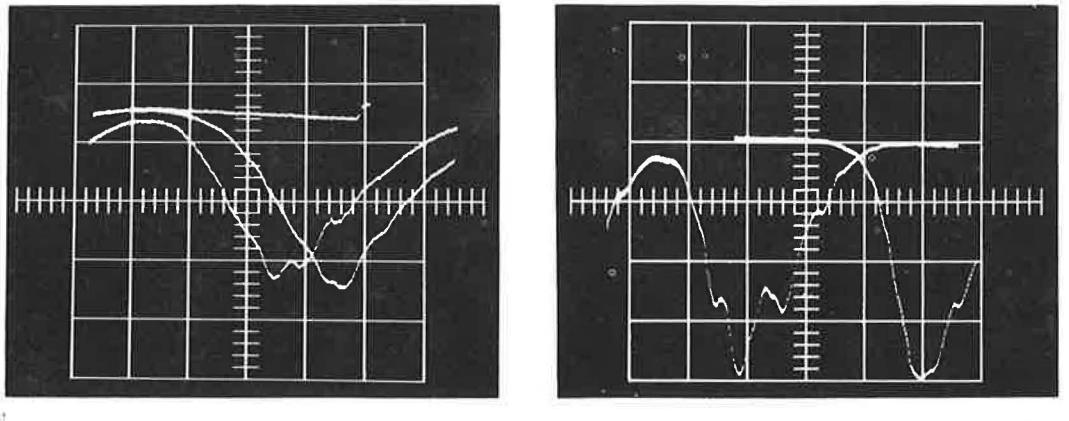

Figure 13. Kinetic response of forward slab corner with low spot: (a) speed = 26.9 ft/sec; and (b) speed = 41.0 ft/sec.

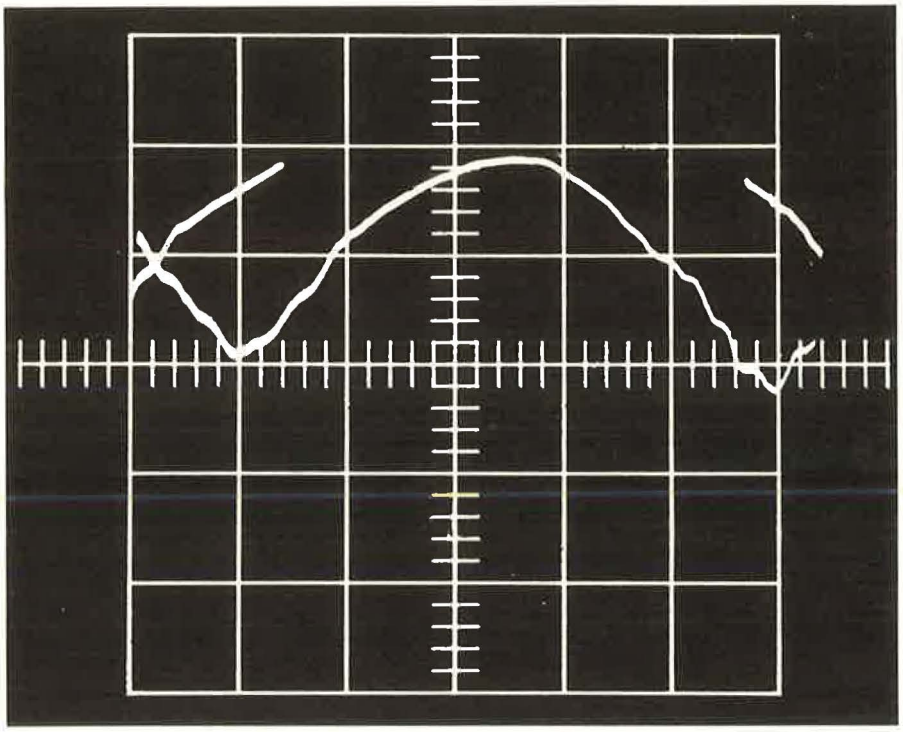

Figure 14. Kinetic response of hind slab corner with low spot (speed = 5.6 ft/sec).

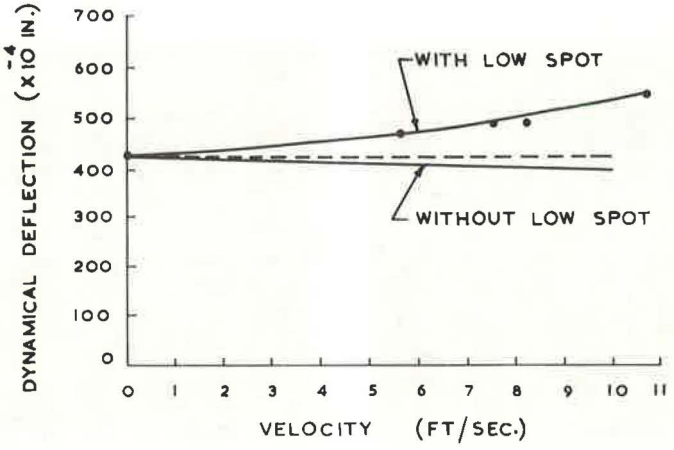

Figure 15. Experimental results of dynamic deflection of hind slab corner (at distance of 1 in. from center of expansion joint) with and without low spot for different load velocities.

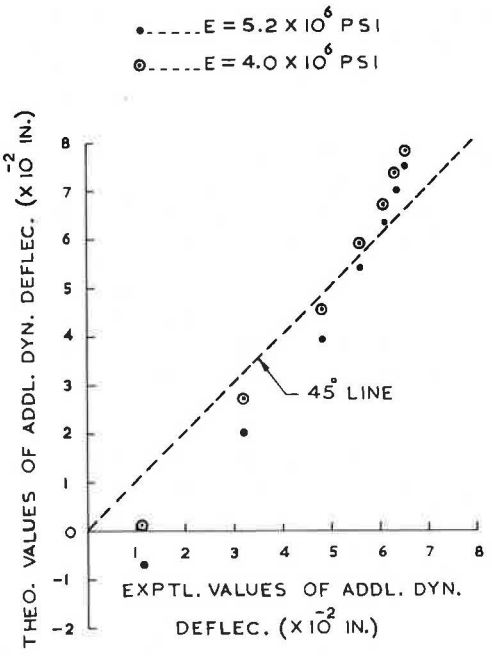

Figure 16. Comparison of theoretical and experimental values of additional dynamic deflection of forward slab.

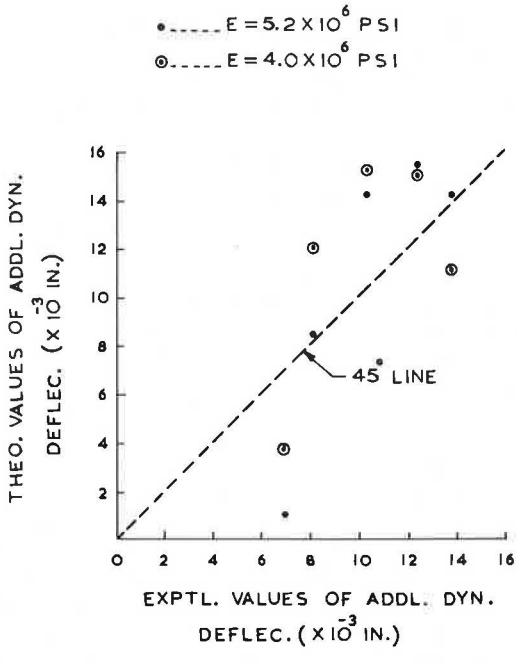

Figure 17. Comparison of theoretical and experimental values of additional dynamic deflection of hind slab.

the joint, Δ_{max} was equal to 0.717 × 0.02419 in. The value of k derived from Eq. 11 was 135,600 lb/in.

Free Period of Vibration—In the relationship $p^2 = kg/\bar{W}$, $\bar{W}$ is the amount of effective load in contact with the low spot causing additional dynamic deflection. With contact area of the front wheel and total area of low spot on the forward slab being 28.7 in.^{2} and 16 in.^{2} respectively, $\bar{W} = 2{,}352 \times {}^{16}/_{28.7} = 1{,}310$ lb. Hence,

$$p = {}^{1}/_{2\pi}\,[(135{,}600 \times 32 \times 12)/1{,}310]^{1/2} \text{ cps}$$

or p is equal to 31.8 cps. Therefore, τ is equal to ${}^{1}/_{31.8}$ sec.

Additional Deflection

Forward Slab—For $\tau = {}^{1}/_{31.8}$ sec, $\tau_1/\tau = 31.8\ \iota/\upsilon$. The values of τ_1/τ were calculated for $\iota = 8$ in. and $\upsilon = 20$ to 50 ft/sec. The values of y/λ and, hence, of y (with $\lambda = 0.10$ in.) could now be obtained either from Eq. 10 or more readily from values shown in Figure 3, taking $\iota' = \iota/2$. The theoretical and experimental values of y, the latter being obtained from the mean curve shown in Figure 12, were compared as shown in Figure 16, which also includes the values for E = 4.0 × 10^6 psi.

Hind Slab—For $\tau_1/\tau = {}^{1}/_{31.8}\ \iota/\upsilon$, $\iota = 8$ in., and $\upsilon = 6$ to 10 ft/sec, the values of τ_1/τ were calculated. From these, the values of y/λ and y could be computed either from Eq. 36 or more readily from values shown in Figure 6, for $\iota' = ({}^{3}/_{8})\ \iota$. The theoretical and experimental values of y are shown in Figure 17.

DISCUSSION AND SUMMARY

1. The objective of the investigation is to determine the additional dynamic deflection of rigid pavement from the impact of a wheel load movement over the low spot in the

corner region of the slab. Readily usable formulas and graphs, which are reported in the paper to determine additional dynamic deflection of both forward and hind slab corners for different conditions of support, allow an easy application of the findings. The theoretically determined values for some selected cases have been compared with the experimental results.

2. The additional deflection is proportional to the depth, length, and slope of low spot, load velocity, and elastic reaction modulus of the slab, depending on support condition. Even though the theoretical curves for additional deflection for both the support conditions (fully supported and unsupported) are similar for either hind or forward slab, those for hind and forward slabs are basically different. The maximum deflection for the forward slab is reached when the load is just leaving the low spot and the vehicle is traveling at high speeds. In the case of the hind slab, the maximum additional deflection at high speeds is always negative, i.e., upward in direction. Positive downward deflection of lower magnitude, however, occurs at lower speeds, and the maximum is induced when the load just leaves the hind slab.

3. For a low spot length over both the hind and forward slabs of 4 to 8 in., slab thickness of 8 in., and effective corner length of 48 in., the maximum positive additional deflections (theoretically determined) in the hind slab do not vary with the length of the low spot and are of the magnitude of 0.415λ and 0.372λ for fully supported and unsupported conditions respectively, where λ is the depth of the low spot. These occur at low speeds of 2.5 to 3.5 ft/sec, 4.5 to 5.5 ft/sec, and 6.5 to 7.5 ft/sec for the 4-, 6-, and 8-in. lengths of the low spot respectively.

4. For the same conditions as in the preceding, the maximum positive deflection (theoretically determined) of the forward slab occurs at a speed of about 70 to 75 ft/sec and approaches the values of 0.96 to 1.0λ and 0.86 to 0.89λ for fully supported and unsupported conditions respectively. The difference between the maximum values for fully supported and unsupported conditions is 0.10 to 0.11λ at high speeds, the deflection in the unsupported slab always being lower in magnitude. When the length of the low spot is increased from 4 to 8 in., the maximum positive deflection is reduced by only 3 to 4 percent.

5. The tests have been conducted on fully supported concrete pavement slabs of a 3.7-in. thickness laid over a W.B.M. subbase (K-value $\approx$ 500 pci). In all the cases within the purview of the tests, there is a gradual reduction in the dynamic deflection with increase in speed of the vehicle when there is no low spot. At a speed of 50 ft/sec (34 mph), the reduction is 27.5 percent when compared to the value at crawl speed (i.e., static condition). With a low spot, the dynamic deflection of the forward slab corner increases very rapidly with speed up to about 50 ft/sec (34 mph), after which the curve is asymptotic. At this speed, the additional positive dynamic deflection due to the low spot is 167 percent of the dynamic deflection when no low spot is present. This amounts to an increase of 94.5 percent in deflection over the static value.

6. The experiment further shows that the dynamic deflection of the hind slab corner also increases with speed of the vehicle when a low spot is present. The increase is 25 and 35 percent over the static condition and the case when no low spot is present respectively for a vehicle speed of 10 ft/sec (6.8 mph). Because, as indicated by theoretical analysis, at high speeds the dynamic deflection of the hind slab corner with a low spot is always lower than it is when no low spot is present, the experiment has been conducted only at low speeds.

7. The comparison of the values of theoretically determined and experimentally obtained additional dynamic deflection shows that they are in good agreement with each other. The agreement in the case of forward slab is, however, more satisfactory. The slight difference between the theoretical and experimental values may be attributed to inaccuracies in theoretical assumptions in the spread and nature of load, value of dynamic modulus of elasticity, K-value of the subbase, and the like. Although in reality the load is of a distributed nature, it has been assumed to be concentrated in the theoretical analysis. There is also the possibility that part of the vibrations of the wheel being transmitted to the body of the vehicle may cause an alteration of the vertical pressure of the springs on the axle. This may happen when the frequency of the wheel is not large in comparison to that of the body of the vehicle.

8. The analysis made in this paper serves to highlight the progressive detrimental effect of the surface irregularities such as low spots on rigid pavement under moving loads and to stress the necessity of exercizing adequate controls during construction of new pavements and proper maintenance of the existing pavement.

ACKNOWLEDGMENT

Acknowledgment is due to B. Subbaraju, Director of the Central Road Research Institute, New Delhi, for his keen interest in pursuit of this study. The paper is published with his permission.

REFERENCES

1. Ghosh, R. K., Lal, R., and Vijayaraghavan, S. R. An Approximate Analysis for Kinetic Response of Triangular Cantilever Overhang. Jour. Australian Road Research Board, Vol. 3, No. 2, June 1967.
2. Taylor, W. H. Concrete Technology and Practice, 2nd Ed. Angus and Robertson Ltd., 1967, p. 218.
3. Timoshenko, S., and Young, D. H. Vibration Problems in Engineering, 3rd Ed. D. Van Nostrand Co., Inc., New York, 1955.
4. Warburton, G. B. The Dynamical Behavior of Structures. Macmillan Co., New York, 1964.
5. Westergaard, H. M. Stresses in Concrete Pavements Computed by Theoretical Analysis. Public Roads, Vol. 7, No. 2, 1926, pp. 25-35.